Desalination and Water Treatment
www.deswater.com
doi: 10.5004/dwt.2019.24330

157 (2019) 349–359
July

Scale formation mechanisms and its control by antiscalants in FO membrane under low temperature conditions

Juyoung Lee, Yongjun Choi, Hyeongrak Cho, Yonghyun Shin, Sangho Lee*

School of Civil and Environmental Engineering, Kookmin University, Jeongneung-Dong, Seongbuk-Gu, Seoul 136-702, Republic of Korea, Tel. +82-2-910-4529; Fax: +82-2-910-4939; emails: sanghlee@kookmin.ac.kr (S. Lee), makrs2@kookmin.ac.kr (J. Lee), choiyj1041@gmail.com (Y. Choi), rhino@kookmin.ac.kr (H. Cho), shinyonghyun@naver.com (Y. Shin)

Received 10 October 2018; Accepted 24 April 2019

ABSTRACT

The performance of forward osmosis (FO) membrane process is generally influenced by the characteristics of the feed and draw solutions. Assuming that FO is applied in cold regions, the temperature of the feed or draw solution may be low, thereby affecting the water productivity and fouling propensity of FO membranes. Unfortunately, little information is available on the capability of FO to low-temperature waters. Accordingly, this study intends to examine the scale formation in FO membrane process under low temperature conditions. Experiments were carried out in a bench-scale experimental set-up using flat sheet commercial FO membrane. The feed temperature was fixed at 25°C and the draw solution temperature was varied from 5°C to 25°C. Mechanisms of scale formation under low-temperature conditions were explored. The effectiveness of antiscalant to control scale formation in FO process was also investigated as a function of draw solution temperature. Results showed that the mechanism of scale formation under low-temperature is different from those under room temperature condition. The comparison of morphologies of the crystals on the FO membrane surfaces revealed the different mechanisms of scale control by the antiscalant under different temperatures.

Keywords: Forward osmosis (FO); Low temperature; Gypsum scaling; Antiscalant; Mechanisms

1. Introduction

Global water shortage is becoming more and more severe all around the world, which results from an increase in population and great development of industries [1]. For this reason, the demand of the seawater desalination and wastewater reuse are rapidly growing, which can supply an ongoing source of fresh water [2,3]. Technologies based on reverse osmosis (RO) are widely used for desalination [4] but they have a serious drawback associated with high energy consumption [5]. The energy costs of the RO process can range from 40% to 60% of the total cost of the RO desalination process [6]. Moreover, in the case of RO, the ability to treat high salinity feeds is limited [7]. In general, RO is not applicable for feeds with total dissolved solids (TDS) greater than 45,000 ppm [8]. Therefore, it is necessary to develop a process that can treat the high salinity feed with lower energy consumption.

Among various technologies for desalination, forward osmosis (FO) process has been recently adopted as a promising alternative to conventional RO processes [9,10]. This is because FO does not rely on hydraulic pressure difference to separate salts from fresh water [11]. Instead, it utilizes the osmotic pressure difference between the draw solution (DS) and feed solution (FS) separated by a semi-permeable membrane. Although FO also has a few limitations, it holds

* Corresponding author.

Presented at the EDS conference on Desalination for the Environment: Clean Water and Energy, 3–6 September 2018, Athens, Greece

potential for applications that do not require draw solute recovery [12]. Osmotic dilution [13] and fertilizer-driven FO [14] are typical examples of such cases. Moreover, FO has higher resistance against membrane fouling caused by particles and organics than RO because there is no hydraulic pressure to compress the foulant layer on the membrane surface [15–17]. Even if the foulant layer forms on FO membranes, it may be easily removed by physical forces due to its relatively loose structures [18].

However, FO is not completely free from problems of membrane fouling, especially if the fouling occurs due to scale formation of sparingly soluble salts such as $CaSO_4$, $CaCO_3$, and silica [19,20]. Unlike particles and organics, the foulant layers formed from scaling are compact and strongly stick to the membrane surface even if there is no or negligible applied hydraulic pressure in FO. Thus, scale formation is a critical problem not only in RO processes but also FO processes as long as the feed water contains such salts [20]. Once scale formation occurs, it leads to a significant flux reduction and thus hinders efficient operation of the process [21]. Accordingly, there have been a lot of researches on the scaling of FO process [19–23].

Fouling due to scale formation has been a critical issue in not only in FO but also in RO processes. It has been reported that there are two distinct mechanisms for scale formation, including surface (heterogeneous) crystallization and bulk (homogeneous) crystallization [24–27]. Techniques for scale control include the modification of feed water properties, adjustment in operating conditions and system design, and use of antiscalant [25]. In fact, antiscalant addition has been accepted as an effective method for mitigating scale formation in RO processes but has not been extensively investigated for FO processes.

Moreover, little information is available on the cases where the temperatures of feed and draw solutions are different in FO processes. A typical situation for such temperature conditions is that FO is applied to treat municipal wastewater by using seawater as the draw solution [11]. Seawater temperature also varies by latitude and moreover there are also many regions where sea water temperature varies from season to season [28]. There are also regions where seawater temperature is close to zero in winter. On the other hand, the wastewater may have higher temperature even in winter because of the heat generation during the wastewater treatment [29]. In this case, there is a temperature difference between feed and draw sides due to the low temperature of the draw solution.

To the best knowledge of the authors in this paper, there is only a handful of studies on the effect of temperatures on FO performance [30]. Moreover, few study focused on the effect of low temperature of draw solution on fouling due to scale formation. Previous researches of scaling of FO membranes were mostly carried out under room temperature or high temperature conditions [30]. Considering the fact that there is an increasing need to apply FO for the treatment of wastewater, which may contain scale forming ions [31,32], it is necessary to understand how FO fouling occurs under low temperature conditions. For this reason, this study focuses on the mechanisms and control of scale formation in FO membrane during the treatment of feed water with scaling potential using low temperature draw solutions.

2. Materials and methods

2.1. FO membrane and module

Commercial FO flat sheet membranes (TORAY chemical, Inc., Seoul, Korea) made of polyamide were used in the experiments. According to the membrane manufacturer, the water permeability A was 6.68 L/m^2 h bar, the salt permeability B was 0.54 L/m^2 h, and the structural parameter S was 0.378 mm, respectively, for the provided FO membranes. Prior to the experiments, the membranes were stored in deionized (DI) water at 4°C after being cut and rinsed with DI water. A laboratory-scale plate and frame membrane module was custom-made, which width, length, and height were 115, 75, and 40 mm, respectively. Two rubber O-rings were used for both feed and draw sides to prevent solution leakage. The effective area of the membrane was 12 cm^2.

2.2. Chemicals and solutions

Special grade sodium chloride (NaCl), sodium hexametaphosphate (SHMP), extra pure grade sodium sulfate (Na_2SO_4), and calcium chloride ($CaCl_2$) were purchased from SAMCHUN PURE CHEMICAL Co. Ltd., (Seoul, Korea). All chemicals were used without additional purification. The draw solution was prepared by dissolving NaCl into DI water and its concentration was 1.0 M. The feed solution was prepared using $CaCl_2{\cdot}H_2O$, Na_2SO_4, and NaCl, the concentrations of which were 13.05, 36, and 5 mM, respectively. The composition of the synthetic feed solution was determined to simulate real industrial wastewater effluent from a steel plant in Korea.

2.3. Bench-scale FO test system

All FO tests were performed using an experimental setup shown in Fig. 1. The flow rate of the draw and feed solution was 0.4 L/min and velocity was 8.33 cm/s, respectively. To maintain the different temperatures of the feed and draw, two heat exchangers were used. The conductivities of feed and draw solutions were monitored using conductivity meters. The flux was calculated by periodically measuring the mass of feed tank using an electronic balance connected to a computer. The operating conditions are described in Table 1.

2.4. FO tests procedure

The FO experiments were performed under different temperatures of the draw solution. The feed temperature was fixed at 25°C and the draw solution temperatures were adjusted to 5(±1)°C, 10(±1)°C, and 25(±1)°C. The temperature of wastewater is usually higher than the surrounding temperature throughout the year due to the heat generation during wastewater treatment. To reflect this, the temperature of the feed solution was set to 25°C as the reference condition. The experiments were carried out in active layer facing on the feed solution (AL-FS) mode and active layer facing on the draw solution (AL-DS) mode and the results were compared. Under AL-FS mode, experiments were conducted until the water flux became less

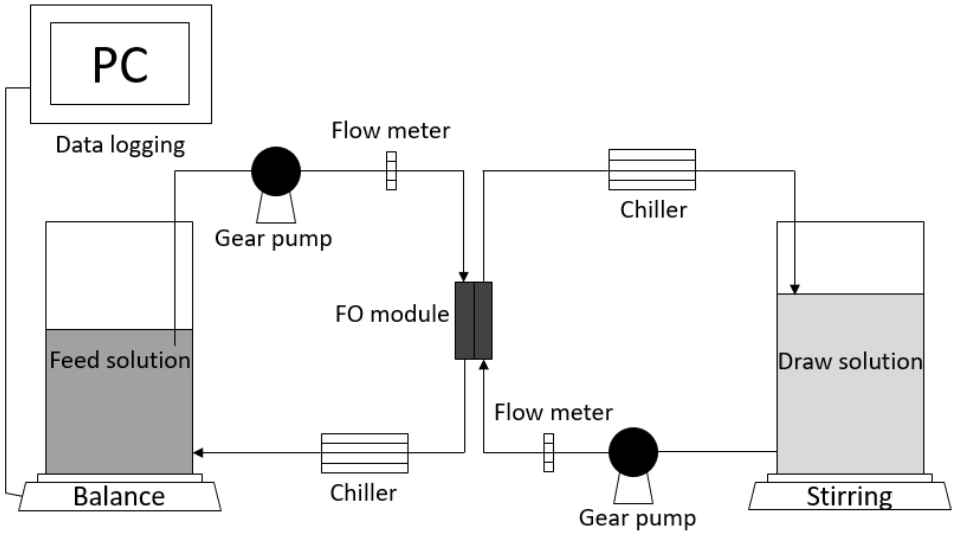

Fig. 1. Schematic diagram of bench-scale FO system.

Table 1
Operating conditions for FO process

Operation type	Forward osmosis (FO) AL-FS/AL-DS mode
Membrane type	Polyamide flat sheet commercial FO membrane
Effective membrane area (cm^2)	12
Feed solution	DI water, $CaCl_2 \cdot H_2O$ 13.05 mM, Na_2SO_4 36 mM, NaCl 5 mM solution, 2 L
Draw solution	NaCl 1 M, 3 L
Flow velocity (cm/s)	8.33
Temperature (°C)	Feed side: 25 (±1)
	Draw side: 5 (±1)/15 (±1)/25 (±1)

than 5 L/m^2 h and in case of AL-DS mode, experiments were terminated when the water flux was maintained at the specific value for more than 36 h.

All FO experiments were performed after insert a membrane coupon into the FO module and conduct the basic performance tests with DI water and 1 M NaCl solution. The feed solution of 2 L and the draw solution of 3 L were used in each test. As a result of our preliminary tests, it was found that the feed volume of 2 L was optimum to carry out FO fouling tests. The temperatures were adjusted with the error of ±1°C. The flux and mass of feed volume were measured after the stabilization of the system for 30 min. At the end of the experiment, all membrane coupons were collected and analysed using a field emission scanning electron microscope (FE-SEM).

3. Results and discussion

3.1. Effect of membrane orientation on fouling due to scale formation

Fig. 2a shows the changes in flux with volume concentration factor (VCF) for FO membranes in AL-FS and AL-DS modes when the temperatures of feed and draw were same at 25°C. Specifically, VCF is calculated by the equation as follows:

$$\mathrm{VCF} = \frac{V_{\mathrm{FS}}}{V_{\mathrm{FS}} - V_P} \tag{1}$$

where V_{FS}, the original feed solution volume, and V_P, the permeate volume that move from feed solution to draw solution by osmotic pressure difference between solutions.

Results showed that the flux decline in the AL-FS mode was less severe than that in the AL-DS mode as demonstrated. In the AL-FS mode, the flux was initially 26 L/m^2 h and decreased with VCF. At the VCF of 1.5, the flux was reduced to 4 L/m^2 h. In the AL-DS mode, the initial flux was 20 L/m^2 h, which was 77% of that in the AL-FS mode. Then, rapid flux decline was observed from the beginning and the flux was less than 5 L/m^2 h after the VCF of 1.05. It is evident from the results that the AL-DS mode resulted in more severe fouling than the AL-FS mode. If there is no membrane fouling, the initial flux of AL-DS orientation is higher than that of AL-FS due to lower degree of internal concentration polarization (ICP) on the draw solution side [9]. However, in this case, the initial flux of AL-DS orientation is lower than that

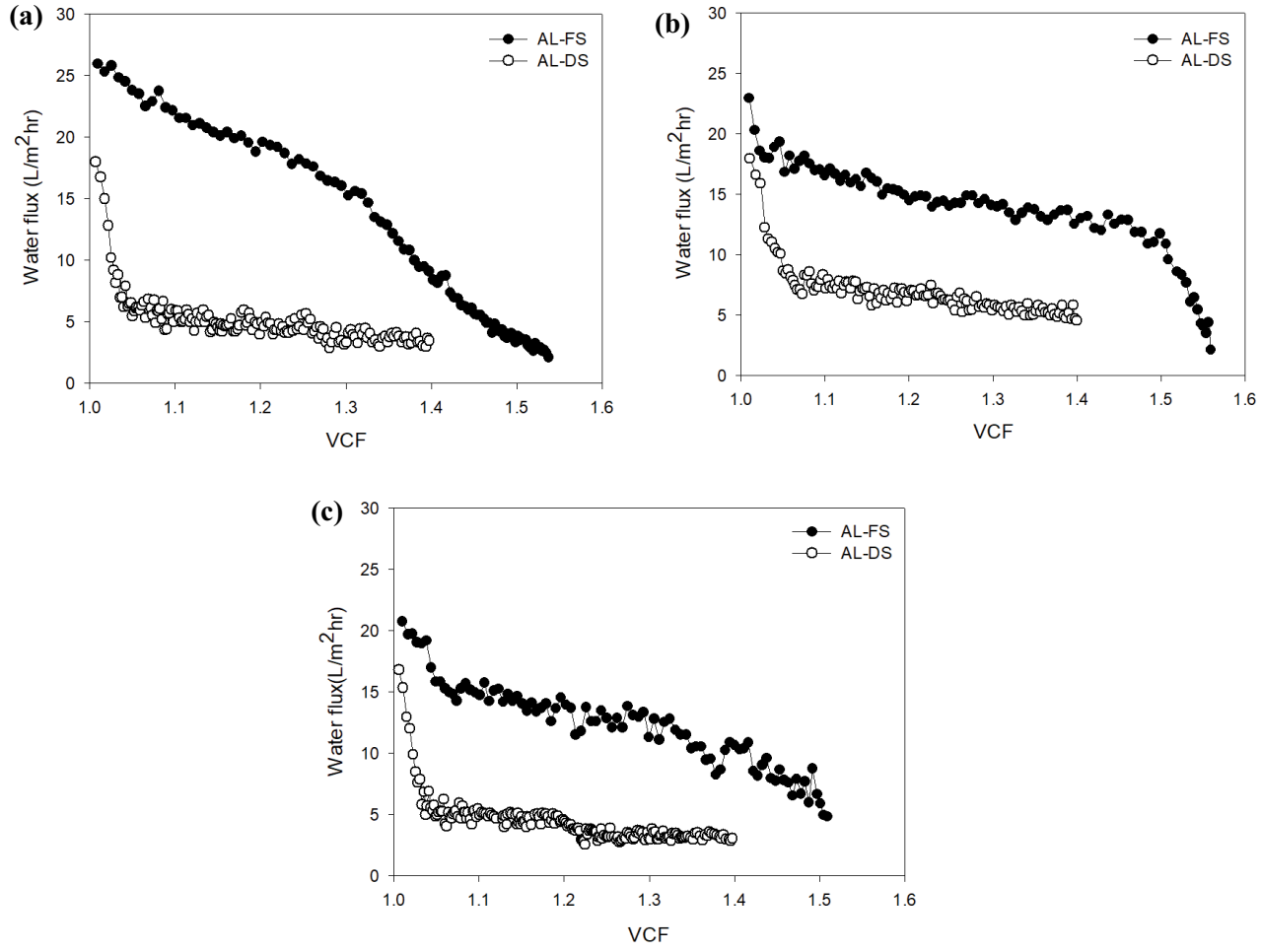

Fig. 2. Dependence of flux on VCF at different draw temperatures in AL-FS and AL-DS modes, (a) draw temperature: 25°C, (b) draw temperature: 15°C, and (c) draw temperature: 5 C.

of AL-FS because rapid membrane fouling occurred from the beginning of the experiments. In fact, the pure water flux was higher in AL-DS orientation (29.75 L/m^2 h) than in AL-FS orientation (27.95 L/m^2 h).

These results are attributed to the different mechanisms of scale formation in the AL-FS and AL-DS modes. As shown in Fig. 4a, fouling occurs in the AL-FS mode through either bulk crystallization or surface crystallization reactions. In bulk crystallization, crystal particles are formed in the bulk phase and deposited onto the membrane surface, leading to a formation of cake layer. In surface crystallization, the nucleation occurs from the active sites on the membrane surface and the lateral growth of the crystals occurs to cover the membrane surface, thereby reducing the effective surface area of the membrane. In both cases, the induction time is required prior to the initiation of the crystallization so the initial rate of crystallization is low. However, the scale formation mechanism in the AL-DS mode is quite different as depicted in Fig. 4b. Since the porous support layer is exposed to the feed solution, crystallization occurs inside the support layer where there is an ICP. The concentrations of $CaSO_4$ are high inside the support layer and thus the crystallization occurs from the beginning. Once the flux is reduced, the ICP also decreases and thus the flux becomes stable. Accordingly, it is strongly recommended to adopt the AL-FS mode to treat feed solution containing scale-forming ions.

3.2. Effect of draw solution temperature on fouling due to scale formation

Fig. 2b shows the flux decline with VCF at the draw solution temperature of 15°C and the feed temperature of 25°C. In the AL-FS mode, flux decline was not serious in the initial phase. Above the VCF of 1.5, a rapid flux decline was observed due to high rate of crystallization above a critical concentration. Similar phenomena were also previously reported [21,22]. Compared with the results in Fig. 2a, it can be found that the initial flux was slightly lower at 15°C than at 25°C. This is attributed to the reduction in the water permeability of the FO membrane and the pore sizes of the support layer of the membrane with a decrease in the draw solution temperature. The rate of flux decline also became lower with a decrease in the draw solution temperature. For instance, when the draw solution temperature was 15°C, the flux was 17 L/m^2 h at VCF of 1.1 and 13 L/m^2 h

at VCF of 1.5, which corresponds to the reduction by 24%. On the other hand, with the draw solution temperature of 25°C, the flux was 22 L/m² h at VCF of 1.1 and 4 L/m² h at VCF of 1.5, which corresponds to the reduction by 82%. Further decrease in the draw solution temperature to 5°C also resulted in a reduction in initial flux and fouling rate as shown in Fig. 2c.

As the temperature of the draw solution decreases, the viscosity increases, which may affect the flux in the FO process. To investigate the viscosity effect, the viscosities of the feed and draw solutions at different temperatures were calculated (Table 2) [33] and compared with the results of FO experiments (AL-FS) using DI water as the feed water (Fig. 3a). The reduction in the FO flux with time was attributed to the dilution of the draw solution with the operation time. The average flux at 25°C of draw solution was 23.8 L/m² h. If the water permeability of the membrane is inversely proportional to the draw solution viscosity, the expected average fluxes at 15°C and 5°C of draw solution should be 20.3 and 15.4 L/m² h, respectively. However, the experiments showed that the measured flux values were 22.8 and 21.1 L/m² h, respectively. This suggests that the dependence of the flux on the draw solution temperature cannot be quantitatively estimated using its viscosity.

This is attributed to the fact that the FO flux is more dependent on the feed temperature than the draw solution temperature. As shown in Fig. 3b, the feed temperature is higher than that of the draw solution. Since the feed temperature was fixed at 25°C, the effective temperature inside the active layer of the membrane may not be significantly different regardless of the draw solution temperature. Accordingly, the flux only weakly depends on the draw solution viscosity. In other words, the effect of draw solution viscosity on the FO fouling in the experiments in Fig. 2 does not seem to be significant.

However, the effect of the draw solution temperature was different in the AL-DS mode. As shown in Figs. 2b and 2c, the flux was not significantly changed even if the draw solution temperature was reduced. In fact, the final flux at 15°C was slightly higher than 25°C and 5°C but the overall behaviors of flux decline were very similar. There may be possible explanations on the higher final flux at 15°C. If the temperature of the draw solution is lower in AL-DS mode, the temperature of the membrane surface also becomes lower. As the membrane surface temperature decreases, the water flux through the membrane may decrease. At the same time, however, the rate of scale formation may also decrease because it is a chemical reaction. Thus, it is hypothesized that the flux at 15°C was the highest due to two competing effects. Increasing the temperature to 25°C resulted in lower flux due to higher scale formation rate. Decreasing the temperature to 5°C also resulted in lower flux due to low water permeability.

Table 2
Dynamic viscosity of feed and draw solutions

Solution type		Temperature (°C)	Dynamic viscosity (cP)
Feed solution	DI water	25	0.892
	Gypsum scaling solution	25	0.899
Draw solution (1 M NaCl solution)		25	1.101
		15	1.290
		5	1.700

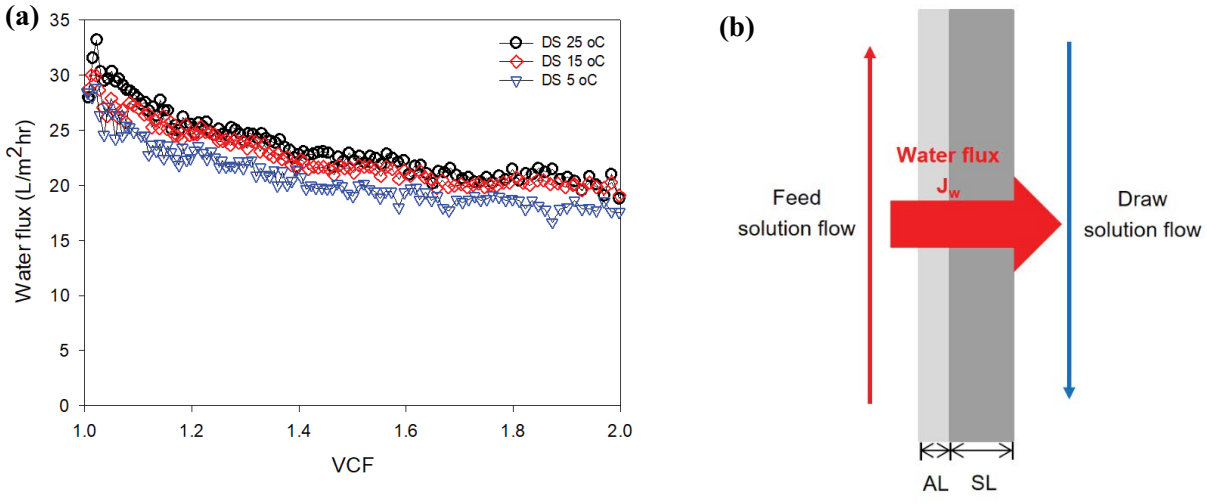

Fig. 3. Effect of viscosity on flux under AL-FS mode at different draw temperature (a), and the pure water transfer mechanism of the FO process under AL-FS mode (b).

As illustrated in Fig. 4b, the fouling due to scale formation in the AL-DS mode occurs in the support layer where the salt concentration is very high due to ICP. Although the rate of scale formation is lower at lower draw solution temperature, it may be still high to cause significant flux decline. In summary, the effect of the draw solution temperature on flux decline is substantial in the AL-FS mode and negligible in the AL-DS mode.

3.3. Effect of antiscalant under low draw solution temperature conditions: AL-FS mode

One of the typical methods to control fouling due to scale formation is the use of antiscalant such as SHMP. The antiscalant molecules are adsorbed into the active sites for the crystal growth, thereby reducing the rate of crystallization. At the same time, the morphology of the crystals may be changed. Fig. 5 compares the variations of flux with VCF at the different SHMP concentrations under different draw solution temperature conditions. The antiscalant was injected to the feed solution. When the draw solution temperature was 25°C (Fig. 5a), the flux increases with an increase in the concentration of SHMP. Due to rapid flux decline, it was difficult to achieve the VCF of 1.6 without the use of SHMP. However, the maximum VCF increased up to 2.7 at the SHMP concentration of 1 mg/L. Increasing the SHMP concentration resulted in higher maximum VCF values: 3.4 at 3 mg/L of SHMP and 3.9 at 5 mg/L of SHMP.

It should be noted that the effect of SHMP on scale inhibition is affected by the draw solution temperature. With the use of SHMP, the flux values at the draw solution temperature of 15°C and 5°C were higher than those at the draw solution temperature of 25°C. As shown in Figs. 5b and c, the initial flux decline was suppressed and the maximum VCF was increased by adding SHMP. It is evident that the improvement of the flux by SHMP was more significant

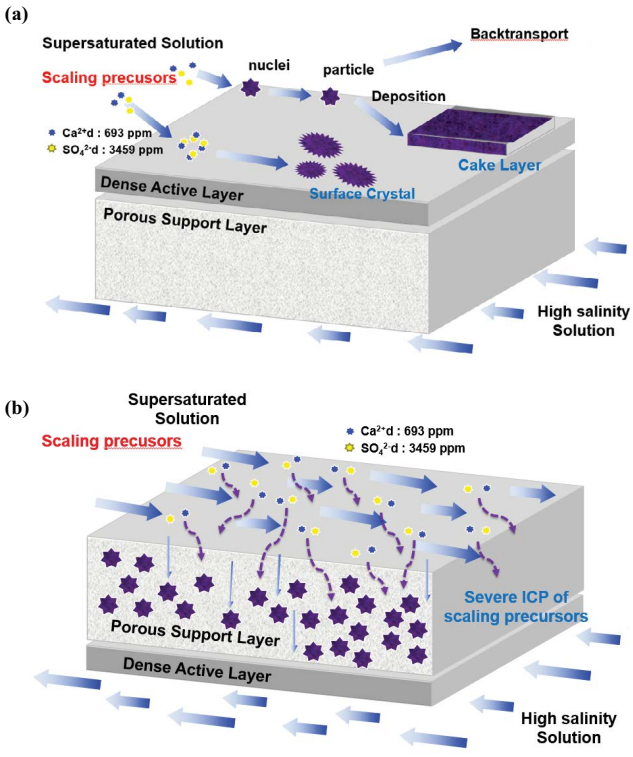

Fig. 4. Proposed mechanisms of fouling due to scale formation in FO membrane (a) AL-FS mode and (b) AL-DS mode.

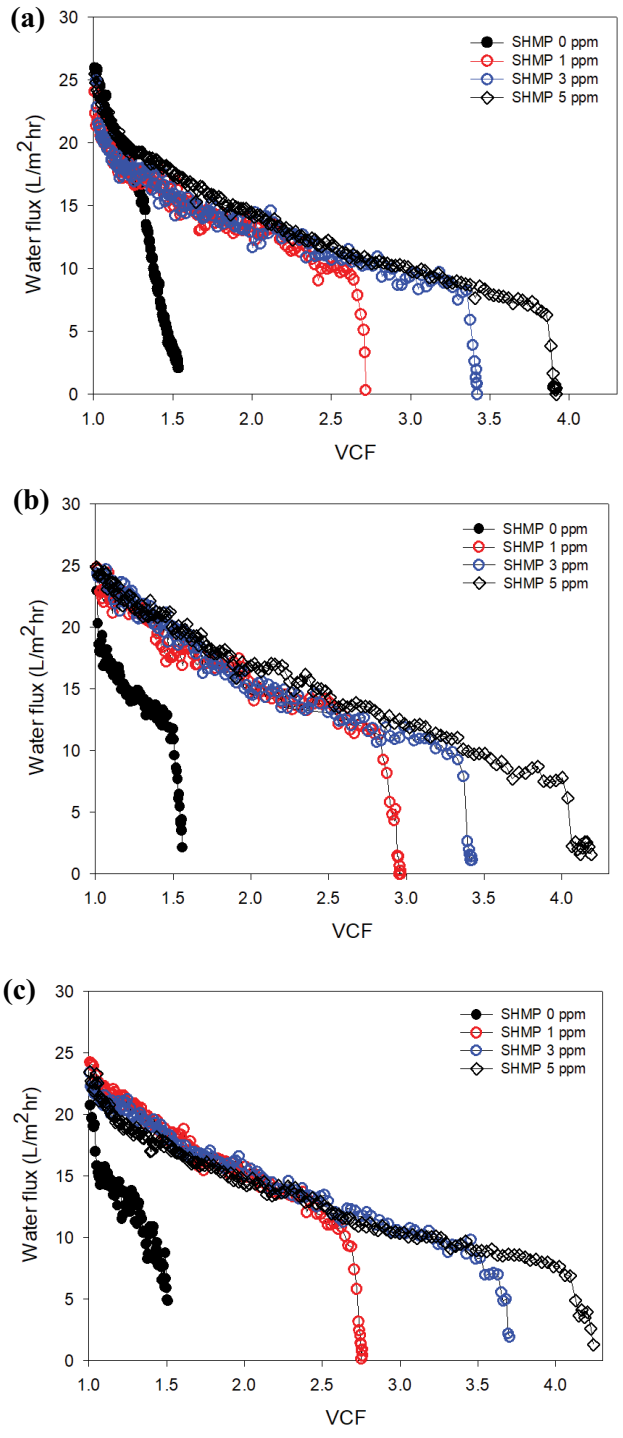

Fig. 5. Effect of SHMP concentration on flux in AL-FS mode at different draw temperatures, (a) draw temperature: 25°C, (b) draw temperature: 15°C, and (c) draw temperature: 5°C.

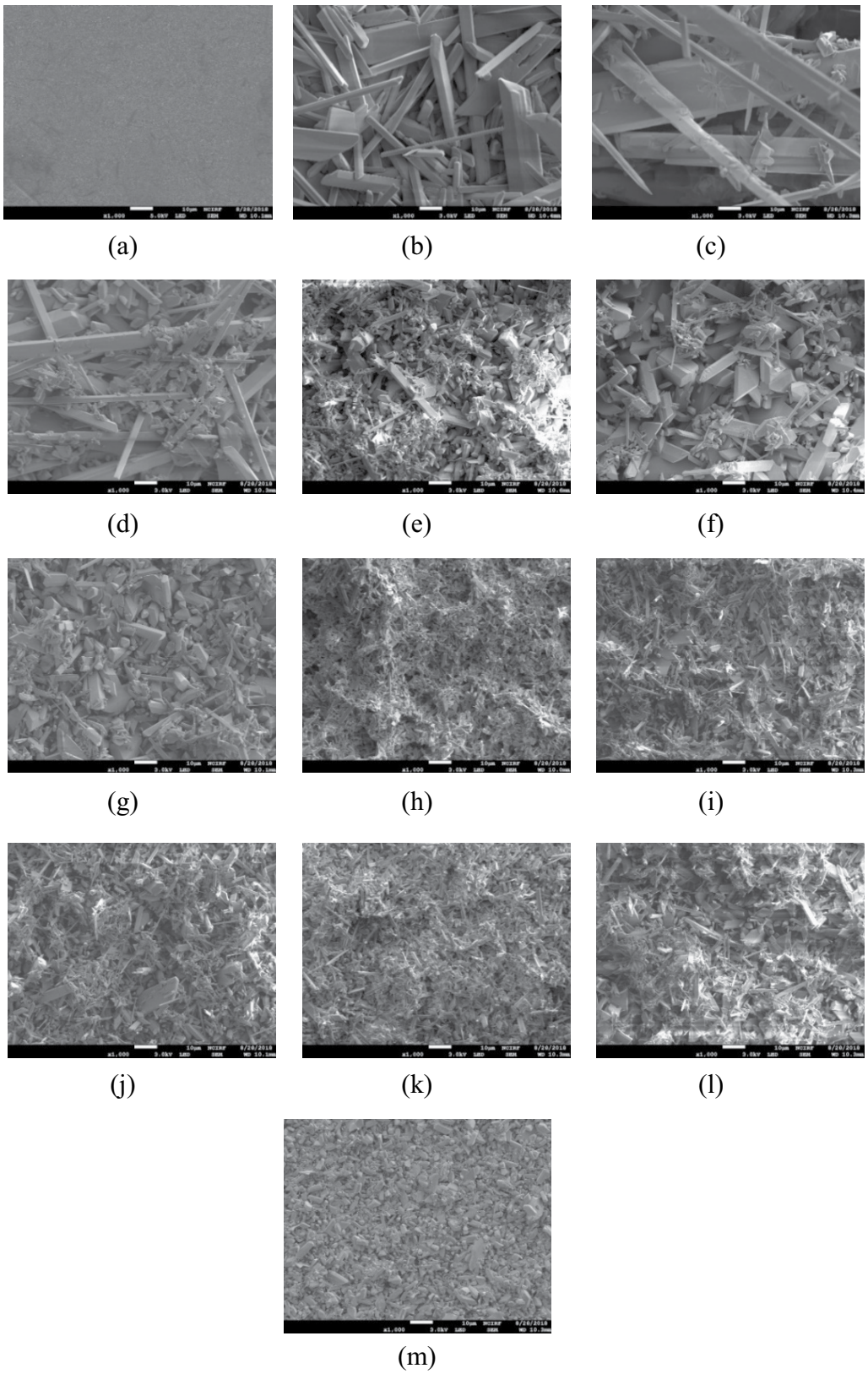

Fig. 6. FE-SEM images of FO membrane surfaces (active layer) (a) intact membrane, (b) DS 25°C – SHMP 0 mg/L, (c) DS 15°C – SHMP 0 mg/L, (d) DS 5°C – SHMP 0 mg/L, (e) DS 25°C – SHMP 1 mg/L, (f) DS 15°C – SHMP 1 mg/L, (g) DS 5°C – SHMP 1 mg/L, (h) DS 25°C – SHMP 3 mg/L, (i) DS 15°C – SHMP 3 mg/L, (j) DS 5°C – SHMP 3 mg/L, (k) DS 25°C – SHMP 5 mg/L, (l) DS 15°C – SHMP 5 mg/L, and (m) DS 5°C – SHMP 5 mg/L. FE-SEM images were taken after surface was magnified 3,000×.

at low temperature conditions (5°C and 15°C) than at the room temperature condition (25°C).

After the FO experiments in the AL-FS mode, the surfaces (active layers) of the membranes were examined using FE-SEM and the results are shown in Fig. 6. The surface (active layer) of the intact membrane is smooth (Fig. 6a). Without the antiscalant, the needle-like crystals were found on the FO membrane surface (Figs. 6b–d). With the addition of SHMP, the shapes of crystals were changed (Figs. 6e–m). The crystals became irregular by the effect of SHMP as reported in the previous studies [19,21,22]. It is likely that the morphologies of the crystals formed at low temperature are different from those at high temperature in the presence of SHMP. For instance, the shapes of crystals at 25°C and 1 mg/L (Fig. 6e) are different from those at lower temperatures (Figs. 6f and g). Similar results were found in the case of 3 mg/L (Figs. 6h–j) and 5 mg/L (Figs. 6k–m) of SHMP concentrations. These results are attributed to the mechanisms of scale control by antiscalants. In fact, antiscalants have properties to distort crystal shapes by interrupting the crystal growth, resulting in the formation of more oval and less compact crystals [22]. Adjustment of the temperature may also affect the shape of crystal by changing crystal growth rates, leading to the scale formation with different shapes.

3.4. Effect of antiscalant under low draw solution temperature conditions: AL-DS mode

A series of experiments were carried out in the AL-DS modes in the presence of SHMP at different draw solution temperatures. Again, the antiscalant was injected to the feed solution. The results are shown in Fig. 7, which clearly indicate the mitigation of fouling by SHMP addition. In all cases, the flux increased with an increase in the SHMP concentration from 0 to 5 mg/L. The initial flux decline was significantly reduced at the SHMP of 5 mg/L. However, the effect of temperature was not clear in the case of the AL-DS mode. For instance, the flux was higher at 15°C (Fig. 7b) than at 25°C (Fig. 7a) in the presence of SHMP. However, the flux was slightly lower at 5°C (Fig. 7c) than at 15°C. This is attributed to the competitive effects that are caused by the temperature change. When the draw solution temperature is reduced, not only the rate of crystallization is reduced but also the rate of scale inhibition by SHMP. If the effect of crystallization rate change is more important, the fouling rate is reduced with a decrease in the draw solution temperature. If the effect of inhibition rate change is more important, the fouling rate increases with a decrease in the draw solution temperature. At the draw solution temperature of 15°C, it seems that the change in the crystallization rate is more important than that in the inhibition rate. On the other hand, at the draw solution temperature of 5°C, it seems that the change in the inhibition rate is more important, leading to a slight increase in the fouling rate in the presence of SHMP.

Fig. 8 shows the FE-SEM images of the surfaces (support layers) of FO membranes after the experiments at the AL-DS mode. The surface of the intact membrane is clean as shown in Fig. 8a. Without the use of antiscalant, the crystals were found on the membrane surface as demonstrated in Figs. 8b–d. However, the amounts of crystals are smaller than those at the AL-FS mode (Figs. 6b–d) even though the flux declines were also significant at the AL-DS mode (Fig. 7).

Fig. 9 shows the FE-SEM images of the cross-section of fouled membranes under AL-DS mode at 25°C draw solution. Compare with virgin membrane, a substantial amount of internal scales were found in both concentration of SHMP 0 and 1 ppm. Based on these FE-SEM images, it

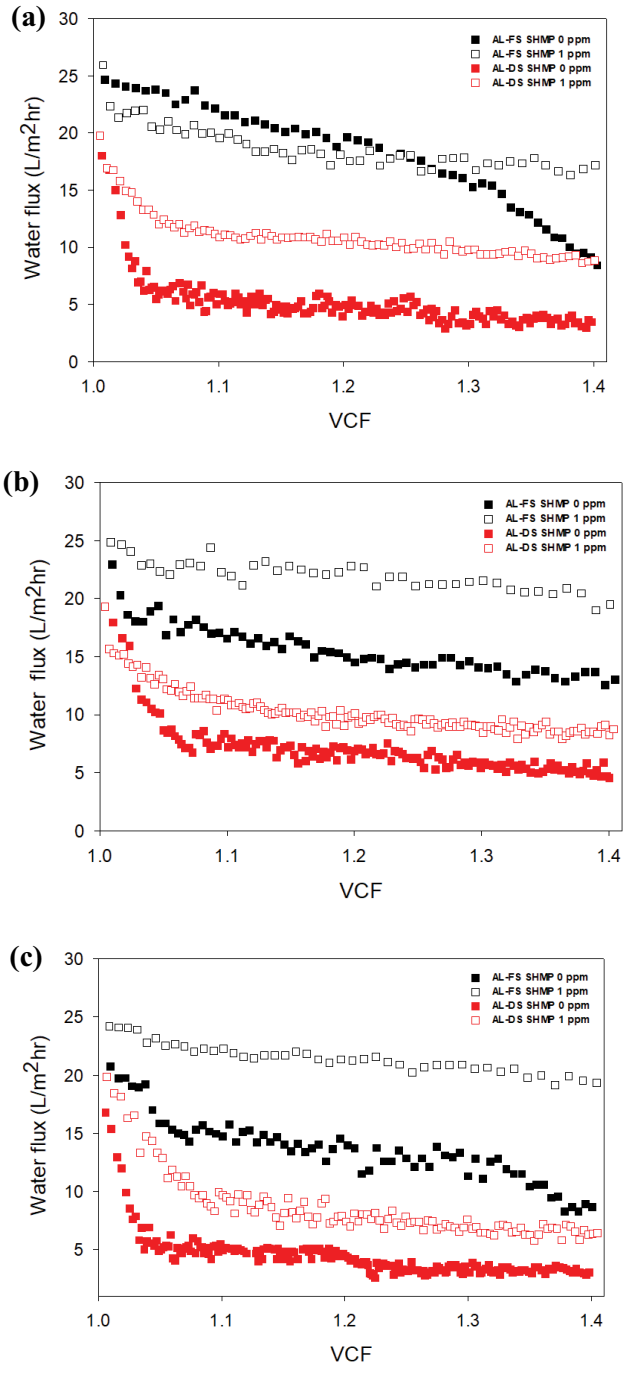

Fig. 7. Effect of SHMP concentration on flux in AL-DS mode at different draw temperatures, (a) draw temperature: 25°C, (b) draw temperature: 15°C, and (c) draw temperature: 5°C.

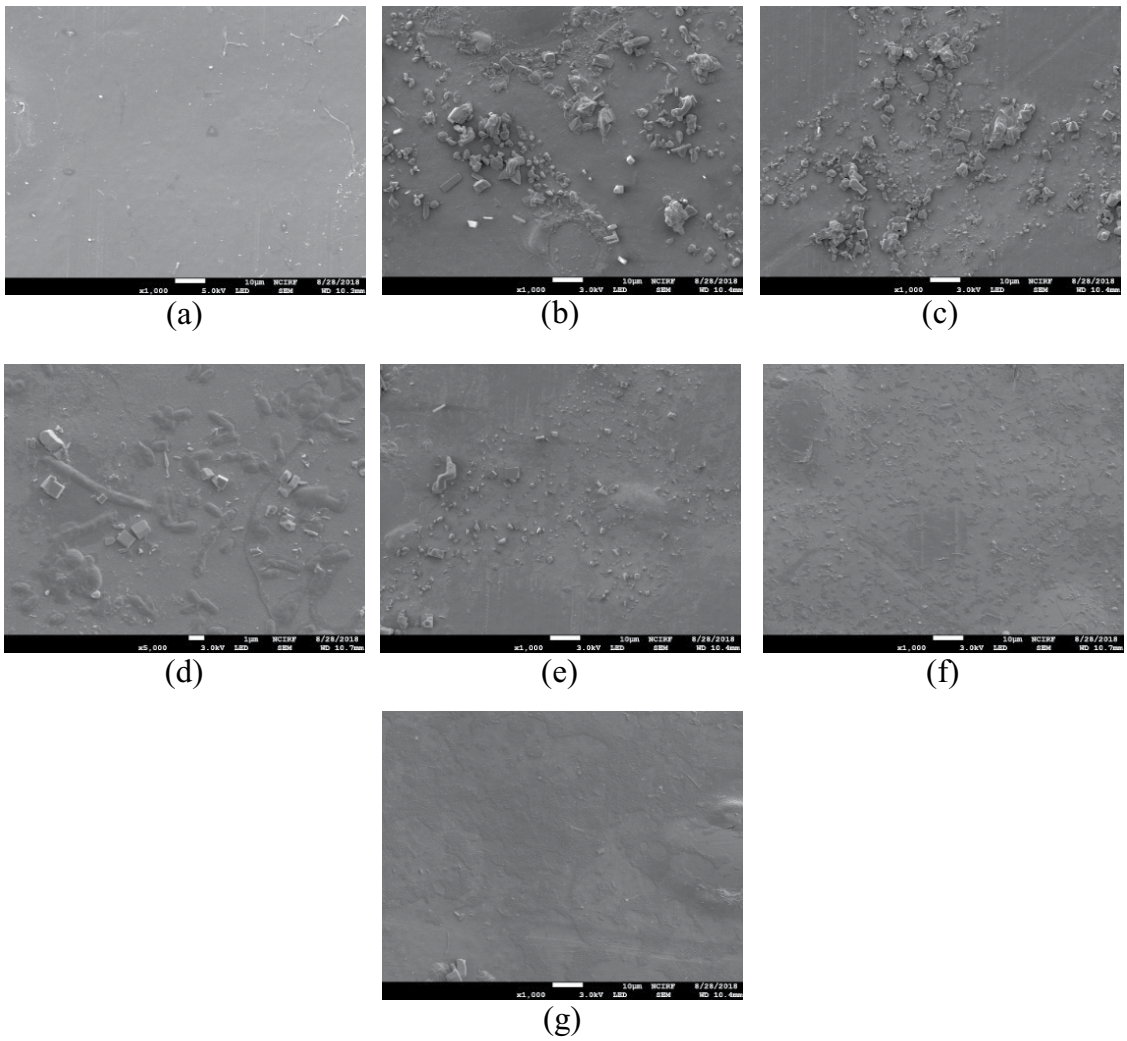

Fig. 8. FE-SEM images of FO membrane surfaces (support layer) (a) virgin, (b) DS 25°C – SHMP 0 mg/L, (c) DS 15°C – SHMP 0 mg/L, (d) DS 5°C – SHMP 0 mg/L, (e) DS 25°C – SHMP 1 mg/L, (f) DS 15°C – SHMP 1 mg/L, and (g) DS 5°C – SHMP 1 mg/L. FE-SEM images were taken after surface was magnified 5,000×.

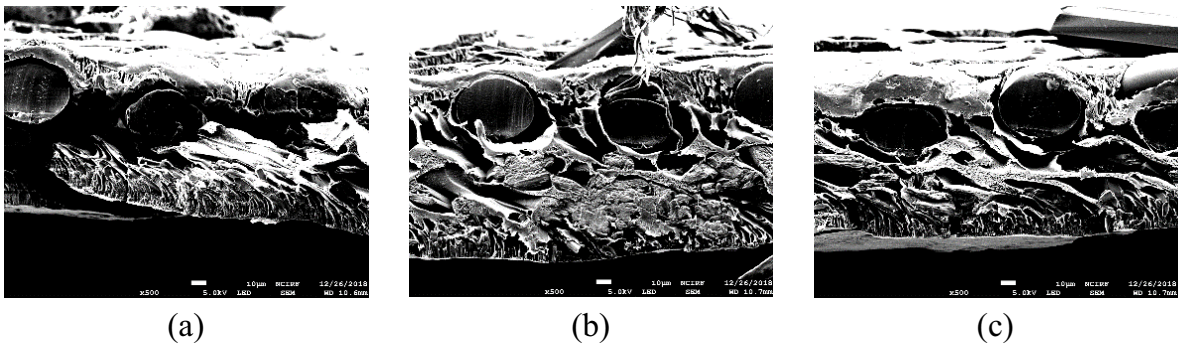

Fig. 9. FE-SEM images of FO membrane cross-sections (AL-DS mode) (a) virgin, (b) DS 25°C – SHMP 0 mg/L, and (c) DS 25°C – SHMP 1 mg/L. FE-SEM images were taken after surface was magnified 500×.

can be confirmed that the scales were also formed inside the membrane support in the AL-DS mode. As already shown in Fig. 4b, the scale formation inside the support layer in the AL-DS mode resulted in the rapid flux decline.

With the addition of 1 mg/L SHMP (Figs. 8e–g), a smaller amounts of crystals was found on the surface of the membranes. Considering the fact that flux decline occurred under these conditions (Fig. 7), it is also likely that significant

amounts of crystals exist inside the porous support layers. The morphologies of the crystals might be changed with a decrease in the draw solution temperature but it was not clearly confirmed due to smaller numbers of crystals found on the membrane surface.

4. Conclusion

In this study, the mechanisms and control of scale formation in FO membrane under low temperature conditions were investigated and the following conclusions were withdrawn:

- The scale formation behaviors of FO membranes were different between the AL-FS and AL-DS modes. More severe fouling was observed in the AL-DS mode than in the AL-FS mode. This is attributed to the different mechanisms of scale formation and ICP.
- The effects of draw solution temperature on the scale formation were different between the AL-FS and the AL-DS mode. In the AL-FS mode, the fouling due to scale formation was mitigated with a decrease in draw solution temperature. In the AL-DS mode, the effect of temperature on fouling due to scale formation was negligible.
- In the AL-FS mode, the inhibition effect of SHMP was affected by the draw solution temperature. A decrease in draw solution temperature resulted in an increased inhibition effect by the SHMP. The morphologies of the crystals formed in the presence of SHMP at low temperature seem to be different from those at high temperature.
- In the AL-DS mode, the effect of temperature on the SHMP effect was not clearly shown. Although flux decline occurred, only a small amount of crystals were found in the presence of SHMP. This suggests that the fouling was caused by the crystals formed inside the support layer of the membrane.

Acknowledgments

This research was supported by Korea Ministry of Environment as "Global Top Project (2017002100001)" and National Research of Korea (NRF-2017M1A2A2047551).

References

[1] W.S. de Amorim, I.B. Valduga, J.M.P. Ribeiro, V.G. Williamson, G.E. Krauser, M.K. Magtoto, J.B.S.O. de Andrade Guerra, The nexus between water, energy, and food in the context of the global risks: an analysis of the interactions between food, water, and energy security, Environ. Impact Assess. Rev., 72 (2018) 1–11.
[2] X. Zheng, D. Chen, Q. Wang, Z. Zhang, Seawater desalination in China: retrospect and prospect, Chem. Eng. J., 242 (2014) 404–413.
[3] State of sea-water desalination technology reviewed, Membr. Technol., 2011 (2011) 9.
[4] Y. Ibrahim, H.A. Arafat, T. Mezher, F. AlMarzooqi, An integrated framework for sustainability assessment of seawater desalination, Desalination, 447 (2018) 1–17.
[5] P. Rao, W.R. Morrow, A. Aghajanzadeh, P. Sheaffer, C. Dollinger, S. Brueske, J. Cresko, Energy considerations associated with increased adoption of seawater desalination in the United States, Desalination, 445 (2018) 213–224.
[6] N. Voutchkov, Energy use for membrane seawater desalination – current status and trends, Desalination, 431 (2018) 2–14.
[7] D. Wu, A. Gao, H. Zhao, X. Feng, Pervaporative desalination of high-salinity water, Chem. Eng. Res. Des., 136 (2018) 154–164.
[8] V.C. Onishi, R. Ruiz-Femenia, R. Salcedo-Díaz, A. Carrero-Parreño, J.A. Reyes-Labarta, E.S. Fraga, J.A. Caballero, Process optimization for zero-liquid discharge desalination of shale gas flowback water under uncertainty, J. Cleaner Prod., 164 (2017) 1219–1238.
[9] Y.-N. Wang, K. Goh, X. Li, L. Setiawan, R. Wang, Membranes and processes for forward osmosis-based desalination: recent advances and future prospects, Desalination, 434 (2018) 81–99.
[10] R.K. McGovern, J.H. Lienhard V, On the potential of forward osmosis to energetically outperform reverse osmosis desalination, J. Membr. Sci., 469 (2014) 245–250.
[11] N.T. Hancock, P. Xu, M.J. Roby, J.D. Gomez, T.Y. Cath, Towards direct potable reuse with forward osmosis: technical assessment of long-term process performance at the pilot scale, J. Membr. Sci., 445 (2013) 34–46.
[12] D.J. Johnson, W.A. Suwaileh, A.W. Mohammed, N. Hilal, Osmotic's potential: an overview of draw solutes for forward osmosis, Desalination, 434 (2018) 100–120.
[13] J.E. Kim, S. Phuntsho, S.M. Ali, J.Y. Choi, H.K. Shon, Forward osmosis membrane modular configurations for osmotic dilution of seawater by forward osmosis and reverse osmosis hybrid system, Water Res., 128 (2018) 183–192.
[14] S. Phuntsho, H.K. Shon, S. Hong, S. Lee, S. Vigneswaran, A novel low energy fertilizer driven forward osmosis desalination for direct fertigation: evaluating the performance of fertilizer draw solutions, J. Membr. Sci., 375 (2011) 172–181.
[15] F.A. Siddiqui, Q. She, A.G. Fane, R.W. Field, Exploring the differences between forward osmosis and reverse osmosis fouling, J. Membr. Sci., 565 (2018) 241–253.
[16] G. Blandin, H. Vervoort, P. Le-Clech, A.R.D. Verliefde, Fouling and cleaning of high permeability forward osmosis membranes, J. Water Process Eng., 9 (2016) 161–169.
[17] E.W. Tow, D.M. Warsinger, A.M. Trueworthy, J. Swaminathan, G.P. Thiel, S.M. Zubair, A.S. Myerson, J.H. Lienhard V, Comparison of fouling propensity between reverse osmosis, forward osmosis, and membrane distillation, J. Membr. Sci., 556 (2018) 352–364.
[18] F. Lotfi, B. Samali, D. Hagare, Cleaning efficiency of the fouled forward osmosis membranes under different experimental conditions, J. Environ. Chem. Eng., 6 (2018) 4555–4563.
[19] M. Zhang, Q. She, X. Yan, C.Y. Tang, Effect of reverse solute diffusion on scaling in forward osmosis: a new control strategy by tailoring draw solution chemistry, Desalination, 401 (2017) 230–237.
[20] Z. Li, R. Valladares Linares, S. Bucs, C. Aubry, N. Ghaffour, J.S. Vrouwenvelder, G. Amy, Calcium carbonate scaling in seawater desalination by ammonia–carbon dioxide forward osmosis: mechanism and implications, J. Membr. Sci., 481 (2015) 36–43.
[21] S. Phuntsho, F. Lotfi, S. Hong, D.L. Shaffer, M. Elimelech, H.K. Shon, Membrane scaling and flux decline during fertiliser-drawn forward osmosis desalination of brackish groundwater, Water Res., 57 (2014) 172–182.
[22] G. Gwak, S. Hong, New approach for scaling control in forward osmosis (FO) by using an antiscalant-blended draw solution, J. Membr. Sci., 530 (2017) 95–103.
[23] B. Mi, M. Elimelech, Silica scaling and scaling reversibility in forward osmosis, Desalination, 312 (2013) 75–81.
[24] S. Lee, J. Kim, C.-H. Lee, Analysis of $CaSO_4$ scale formation mechanism in various nanofiltration modules, J. Membr. Sci., 163 (1999) 63–74.
[25] M. Shmulevsky, X. Li, H. Shemer, D. Hasson, R. Semiat, Analysis of the onset of calcium sulfate scaling on RO membranes, J. Membr. Sci., 524 (2017) 299–304.
[26] A.J. Karabelas, A. Karanasiou, S.T. Mitrouli, Incipient membrane scaling by calcium sulfate during desalination in narrow spacer-filled channels, Desalination, 345 (2014) 146–157.
[27] S. Lee, R.M. Lueptow, Control of scale formation in reverse osmosis by membrane rotation, Desalination, 155 (2003) 131–139.

[28] K.M. Sassi, I.M. Mujtaba, Effective design of reverse osmosis based desalination process considering wide range of salinity and seawater temperature, Desalination, 306 (2012) 8–16.
[29] F. Kretschmer, L. Simperler, T. Ertl, Analysing wastewater temperature development in a sewer system as a basis for the evaluation of wastewater heat recovery potentials, Energy Build., 128 (2016) 639–648.
[30] M.R. Chowdhury, J.R. McCutcheon, Elucidating the impact of temperature gradients across membranes during forward osmosis: coupling heat and mass transfer models for better prediction of real osmotic systems, J. Membr. Sci., 553 (2018) 189–199.
[31] R. Thiruvenkatachari, M. Francis, M. Cunnington, S. Su, Application of integrated forward and reverse osmosis for coal mine wastewater desalination, Sep. Purif. Technol., 163 (2016) 181–188.
[32] G. Gwak, D.I. Kim, S. Hong, New industrial application of forward osmosis (FO): precious metal recovery from printed circuit board (PCB) plant wastewater, J. Membr. Sci., 552 (2018) 234–242.
[33] K.G. Nayar, M.H. Sharqawy, L.D. Banchik, J.H. Lienhard V. Thermophysical properties of seawater: a review and new correlations that include pressure dependence, Desalination, 390 (2016) 1–24.